PNAS RESEARCH ARTICLE | IMMUNOLOGY AND INFLAMMATION

The neuroimmune CGRP–RAMP1 axis tunes cutaneous adaptive immunity to the microbiota

Warakorn Kulalert[a,1], Alexandria C. Wells[a,2], Verena M. Link[a,2], Ai Ing Lim[a], Nicolas Bouladoux[a,b], Motoyoshi Nagai[a], Oliver J. Harrison[a], Olena Kamenyeva[c], Juraj Kabat[c], Michel Enamorado[a,d], Isaac M. Chiu[e], and Yasmine Belkaid[a,b,f,1]

Contributed by Yasmine Belkaid; received December 27, 2023; accepted January 22, 2024; reviewed by Iliyan Iliev and Phillip Scott

The somatosensory nervous system surveils external stimuli at barrier tissues, regulating innate immune cells under infection and inflammation. The roles of sensory neurons in controlling the adaptive immune system, and more specifically immunity to the microbiota, however, remain elusive. Here, we identified a mechanism for direct neuroimmune communication between commensal-specific T lymphocytes and somatosensory neurons mediated by the neuropeptide calcitonin gene–related peptide (CGRP) in the skin. Intravital imaging revealed that commensal-specific T cells are in close proximity to cutaneous nerve fibers in vivo. Correspondingly, we observed upregulation of the receptor for the neuropeptide CGRP, RAMP1, in $CD8^+$ T lymphocytes induced by skin commensal colonization. The neuroimmune CGRP–RAMP1 signaling axis functions in commensal-specific T cells to constrain Type 17 responses and moderate the activation status of microbiota-reactive lymphocytes at homeostasis. As such, modulation of neuroimmune CGRP–RAMP1 signaling in commensal-specific T cells shapes the overall activation status of the skin epithelium, thereby impacting the outcome of responses to insults such as wounding. The ability of somatosensory neurons to control adaptive immunity to the microbiota via the CGRP–RAMP1 axis underscores the various layers of regulation and multisystem coordination required for optimal microbiota-reactive T cell functions under steady state and pathology.

neuroimmune crosstalk | T cells | microbiota | CGRP

Significance

Multisystem coordination at barrier surfaces is critical for tissue functions and integrity, in response to microbial and environmental cues. In this study, we identified a neuroimmune crosstalk mechanism between the sensory nervous system and the adaptive immune response, mediated by the neuropeptide CGRP (calcitonin gene–related peptide) and its receptor RAMP1 on skin microbiota–induced T lymphocytes. The neuroimmune CGPR-RAMP1 axis constrains adaptive immunity to the microbiota and overall limits the activation status of the skin epithelium, impacting tissue responses to wounding. Our study opens the door to a broad avenue to modulate adaptive immunity to the microbiota utilizing neuromodulators, allowing for a more integrative and tailored approach to harnessing microbiota-induced T cells to promote barrier tissue protection and repair.

Mammalian neural and immune cells are constantly exposed to external stimuli at barrier surfaces, and therefore have evolved to sense and respond to fluctuating environmental cues present in the tissue milieu. Correspondingly, to achieve such common sentinel goals, the nervous and immune systems communicate largely with shared signaling molecules such as cytokines, chemokines, and neuropeptides, blurring the discrete functional partitioning between these two critical biological units (1–3). Neuroimmune crosstalk, which can have multifaceted consequences on the barrier tissues, has thus emerged as a crucial research area that could result in a more holistic understanding of tissue physiology and pathology, as well as novel therapeutic avenues in the context of local infection and tissue inflammation (4–6).

While neuroinflammation in neurodegeneration, in particular those involving the central nervous system and devastating neurological diseases in humans, have been well-characterized (7–9), exhaustive examination of neuroimmune interaction in the peripheral tissues remains at its early stage. Of note, regulation of tissue immunity by the autonomic nervous system including sympathetic, parasympathetic, or enteric neurons, in particular in the context of anti-inflammatory reflex, has been documented (10, 11). What remains to be further characterized are any direct immunological roles of somatosensory fibers, in particular the abundant nociceptive and/or peptidergic neuronal subsets (12) that integrate external stimuli ranging from gentle touch to noxious pain at barrier sites. Our specific goal of this study is to examine how such nerve fibers, highly enriched in the skin, directly engage immune cells at homeostasis at this largest barrier site and organ.

Seminal studies have revealed that innate immune cells such as neutrophils and dendritic cells can be regulated by molecular mediators associated with the nervous system such as the neuropeptide CGRP (calcitonin gene–related peptide) in the context of bacterial and fungal infection (13–16) and skin inflammation (17, 18), often involving pain sensation (19). Innate lymphoid cells, such as ILC2s in the lung and the intestine, have also been shown to respond to CGRP in the context of parasitic infection (20–22). Substance P, another critical neuropeptide secreted by sensory fibers, can regulate immune cells involved in allergy such as mast cells (23) and dendritic cells (24). Optogenetic activation of cutaneous nociceptors can elicit inflammation termed anticipatory Type 17 immune response in the skin (25). What remains unclear is whether somatosensory neurons at barrier sites

Author contributions: W.K. and Y.B. designed research; W.K., A.C.W., V.M.L., A.L., N.B., M.N., O.J.H., O.K., and M.E. performed research; I.M.C. contributed new reagents/analytic tools; W.K., A.C.W., V.M.L., and J.K. analyzed data; and W.K. and Y.B. wrote the paper.

Reviewers: I.I., Weill Cornell Medicine; and P.S., University of Pennsylvania.

The authors declare no competing interest.

[1]To whom correspondence may be addressed. Email: kulalertw2@nih.gov or yasmine.belkaid@pasteur.fr.

[2]A.C.W. and V.M.L. contributed equally to this work.

This article contains supporting information online at https://www.pnas.org/lookup/suppl/doi:10.1073/pnas.2322574121/-/DCSupplemental.

Published March 7, 2024.

can directly control long-lasting and highly specific adaptive immune cells, particularly under homeostasis, in the absence of any infection or apparent tissue inflammation.

The skin is colonized by the microbiota, which in turn plays a fundamental role in educating and regulating host adaptive immune cells to maintain barrier tissue homeostasis (26, 27). For instance, the human skin commensal *Staphylococcus epidermidis* robustly induces accumulation of T lymphocytes that harbor diverse functions beneficial to the mammalian host including tissue repair and antimicrobial defense under steady state, without any manifestations of inflammation or infection (28–32). Because these functionally unique and versatile commensal-specific T cells are situated in tissues that are highly innervated, it is crucial to understand the extent to which microbiota-reactive T cells interact with and are controlled by somatosensory nerves in the barrier tissues. In this study, we identified a mechanism by which sensory neurons directly regulate commensal-reactive T cells via the neuropeptide CGRP and its cognate receptor RAMP1 on T cells in the skin. The neuroimmune CGRP–RAMP1 axis functionally tunes commensal-specific T cells to constrain Type 17 responses and control T cell activation status under steady state, with functional consequences upon overall tissue activation and responses to insults, demonstrating the direct regulation of homeostatic adaptive immunity by sensory neurons, shaping barrier tissue physiology in the milieu enriched with a diverse array of microbes and sensory modalities.

Results

Commensal-Specific T Cells Are in Close Proximity to Sensory Nerve Fibers in the Skin at Homeostasis. To assess cutaneous neuroimmune crosstalk, we first examined whether there was a physical association between commensal-reactive T lymphocytes and somatosensory fibers innervating the skin. To this end, the skin of specific-pathogen free mice was colonized topically with a new commensal microbe, *S. epidermidis*, inducing an accumulation of commensal-reactive $CD8^+$ T cells without any manifestations of inflammation (28, 33). After topical association with the commensal, we employed confocal microscopy to visualize microbiota-reactive, polyclonal $CD8^+$ T cells that accumulated in the mouse skin, and observed that these T cells were in close proximity to sensory nerve peripherals, with some in direct physical contact with the sensory fibers (Fig. 1*A*), suggesting a potential functional neuroimmune interaction at this barrier tissue under steady state.

To further study the dynamic interaction between commensal-specific T cells and sensory nerve fibers in vivo, we utilized intravital 2-photon microscopy. Mice carrying a reporter for sensory fibers (*Calca-EGFP*) (34) were adoptively transferred with T-cell receptor (TCR) transgenic *S. epidermidis*-specific $CD8^+$ T cells ($Bowie^{Tg}$) and topically associated with the commensal. Following topical association, $Bowie^{Tg}$ T cells were in close proximity to sensory nerves, with an average distance of 4.9 ± 5.6 μm over a defined intravital recording period in vivo. Notably, a substantial portion (over 32%) of the $Bowie^{Tg}$ cells were in direct contact (0 μm) with the neural fibers (Fig. 1 *B* and *C* and Movie S1). In contrast, the $Bowie^{Tg}$ T cells were comparatively distant to the vasculature over the same intravital recording period, with an average distance 24.6 ± 13.2 μm (Fig. 1*C*). Overall, the $Bowie^{Tg}$ T cells were evenly distributed spatially in relation to the endothelia over the in vivo recording period (low skewness of 0.1, with median distance of 25 μm), in contrast with the T cell–nerve distance distribution that was skewed toward direct contact (high skewness of 1.7, with median distance of 3.25 μm) over the recording period (Fig. 1*C*). Of note, we previously reported a significant physical interaction between commensal-specific T cells and somatosensory nerve peripherals in $CD4^+$ T cells induced by another skin commensal bacterium, *Staphylococcus aureus* (32), suggesting that neuroimmune interaction may be an evolutionarily conserved feature for conventional αβ T cells induced by a broad array of commensal microbes at the barrier site under steady state.

T cell shape and motility have been associated with antigen-mediated signal strength (35) and activation status (36). We thus asked whether physical proximity to sensory nerve fibers could impact commensal-specific T cell behavior in vivo. Following *S. epidermidis* association, T cells that were in direct contact with the sensory fibers (distance = 0 μm) exhibited lower sphericity in morphology than those situated further from the nerves (distances > 0 μm) over the intravital recording period (Fig. 1 *D*, *Left*). Our observations point to the potential ability of sensory fibers to influence T cell functions, as T cells that are distant from the sensory fibers tend to manifest rounding, associated with heightened activation status (36). This correlation between physical proximity and cellular shape in vivo, while prominent in the context of the nerve-T cell interface, was not evident in the context of the vasculature-T cell interface (*SI Appendix*, Fig. S1). Furthermore, this unique in vivo relationship between T cell–nerve interaction and cellular shape was also observed in commensal-specific $CD4^+$ T cells upon topical colonization by another commensal *Staphylococcus* species, *S. aureus* (Fig. 1 *D*, *Right*) under steady state, indicating that such manifestation of neuroimmune coordination may be an evolutionarily conserved feature in the context of homeostatic immune response to a broad range of commensals, and may confer functional consequences in the tissue under homeostasis.

Taken together, these observations of intimate physical neuroimmune interaction motivated us to further address whether the sensory nervous system could directly regulate commensal-induced lymphocytes.

Skin Commensal–Induced T Cells Upregulate RAMP1, the Receptor for Neuropeptide CGRP. Our observations that commensal-specific T cells were closely associated with sensory nerve peripherals raised mechanistic questions underlying the neuroimmune crosstalk in the skin. We thus examined whether commensal-specific T cells expressed any molecular machinery that equipped them with the potential ability to respond to neuronally derived signals such as neuropeptides. Unbiased transcriptomic analysis revealed that a *S. epidermidis*–induced population of $CD8^+$ T cells (Tc17: $CCR6^+$ $CD8^+$) exhibited a significant transcriptional upregulation of the *Ramp1* gene encoding the receptor for neuropeptide CGRP [Fig. 2*A*, RNA-seq (RNA-sequencing) dataset from our laboratory (29)]. In contrast, naïve and antigen-experienced (T_{EM}) $CD8^+$ T cells isolated from the skin-draining lymph nodes of commensal-colonized animals did not exhibit any significant induction of *Ramp1* (Fig. 2*A*). Of note, in our examination of over 100 neuronal genes expressed in diverse skin $CD8^+$ T cell populations, we observed upregulation of a number of neuropeptide, neurotrophic factor or neuroendocrine signaling-related genes (*Ramp1, Ramp3, Ntrk3, Calca, Gch1, Nr3c1,* and *Bex3*) in commensal-induced Tc17 cells, compared to $CD8^+$ T cells induced under infection (*SI Appendix*, Fig. S2*A*). These data suggest a wide range of signaling molecules that could be associated with neuronal control of adaptive immunity to commensals, with *Ramp1* being the most induced neuroimmune mediator gene candidate. Upregulation of *Ramp1* was unique to commensal-induced Tc17 cells, as *Ramp1* expression was modest

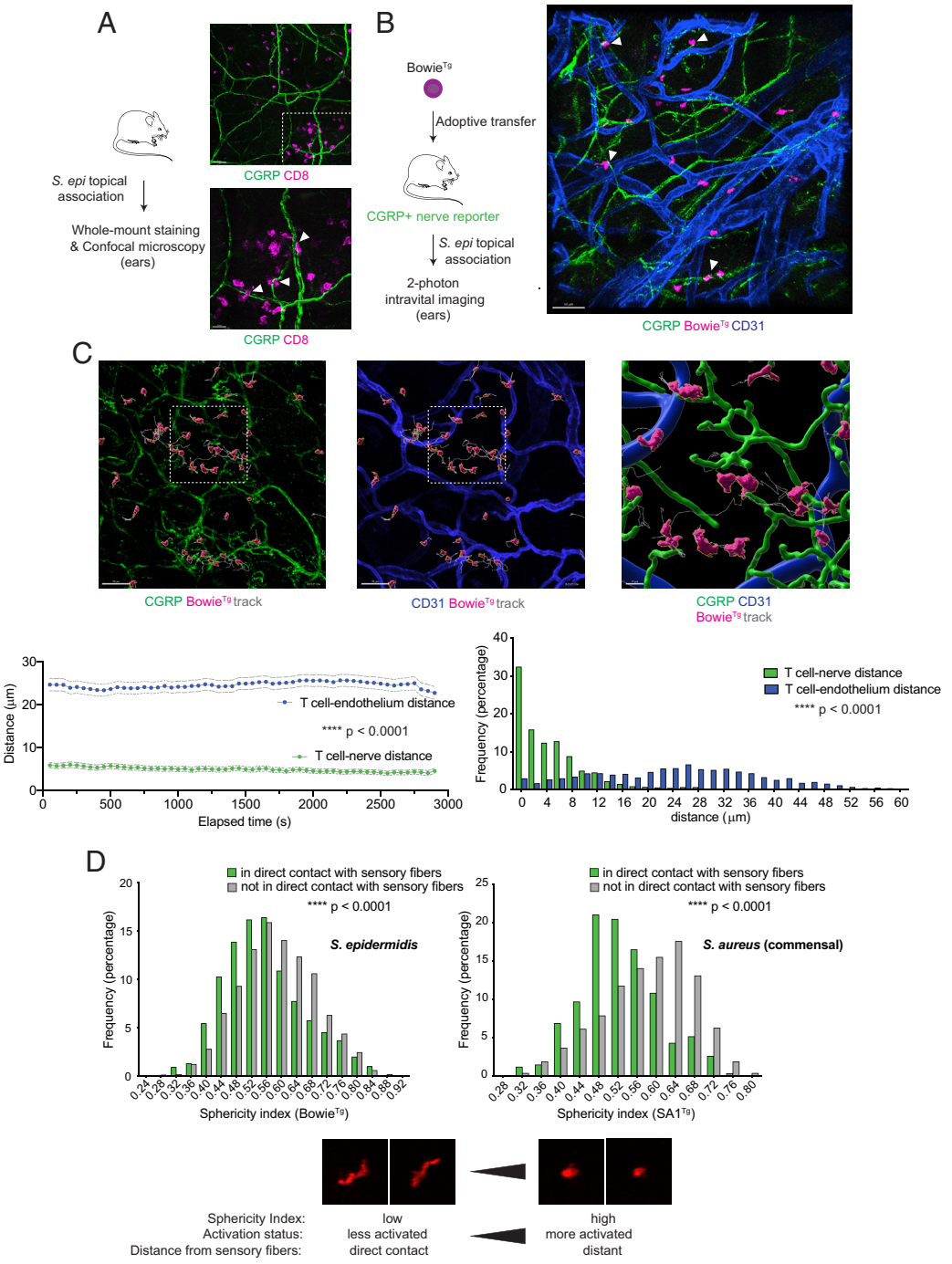

Fig. 1. Commensal-specific T lymphocytes are in close proximity to sensory nerve fibers in the skin in vivo. (*A*) SPF C57BL/6 mice were topically associated with *S. epidermidis* isolate LM087 in Tryptic Soy Broth (TSB) every other day for four times. Fourteen days after the initial association, mouse ears were fixed and stained for CGRP+ sensory neurons (anti-CGRP isoform α; green) and $CD8^+$ T cells (anti-CD8α; magenta). Unassociated ears do not have $CD8^+$ T cell accumulation, and therefore $CD8^+$ T cells accumulating in the skin shown were induced by new commensal colonization. The *Bottom* panel depicts magnification of a region demarcated by white dash lines in the *Top* panel. White scale bars represent 50 μm (*Bottom Left* corner of *Top* panel) and 20 μm (*Bottom Left* corner of *Bottom* panel). Arrowheads indicate direct contact between T cells and nerve fibers. (*B*) Adoptive transfer of OFP^+ *S. epidermidis*-specific transgenic T cells ($Bowie^{Tg}$; magenta) was performed on albino SPF C57BL/6 hosts harboring the *Calca-EGFP* reporter (marking $CGRP^+$ sensory fibers; green) prior to intravital imaging. Anti-CD31 (marking the vasculature; blue) injection was performed prior to imaging. A white scale bar (*Bottom Left*) represents 50 μm. Arrowheads denote direct contact between commensal-specific $CD8^+$ T cells and $CGRP^+$ sensory fibers. (*C*) Each image panel represents the same visual field, with the same experimental approach and color schematic described in (*B*). Note the gray track representing dynamic in vivo T cell motility/displacement over the recording period, shown in Movie S1. The 3D cartoon rendering in the *Rightmost* panel represents magnification of the region demarcated by white dashed lines in the *Leftmost* and *Middle* panels. Graphs represent quantitation of shortest distances between the T cells and the indicated neural or endothelial structures. Each data point in the *Left* graph represents an average distance between T cells and respective structures at each elapsed time point, with SD shown in dashed lines. The *Right* graph is a histogram, illustrating the distribution of distances between T cells and respective structures over the recording period. Statistical significance was determined using all distance values over the defined recording period, comparing the T cell–nerve distance values with the T cell–endothelium distance values. (*D*) Each graph represents distribution of cellular sphericity indexes of commensal-specific T cells ($Bowie^{Tg}$ for *S. epidermidis* and $SA1^{Tg}$ for *S. aureus*) over the recording period. Bars in the indicated colors represent populations of the T cells that are in direct contact or not in direct contact with sensory fibers. Statistical significance was determined using all sphericity index values over the defined recording period, comparing the population that was in direct contact with the nerve fibers vs. the population that was not in direct contact with the nerve fibers. The *Bottom* schematic shows representative images of the cells with the indicated range of sphericity values and summarizes the relationship between distances from nerve fibers and sphericity and potential activation status. All data shown in (*A–D*) represent at least three independent experiments. ****$P < 0.0001$ as calculated with Student's *t* test. See also *SI Appendix*, Fig. S1.

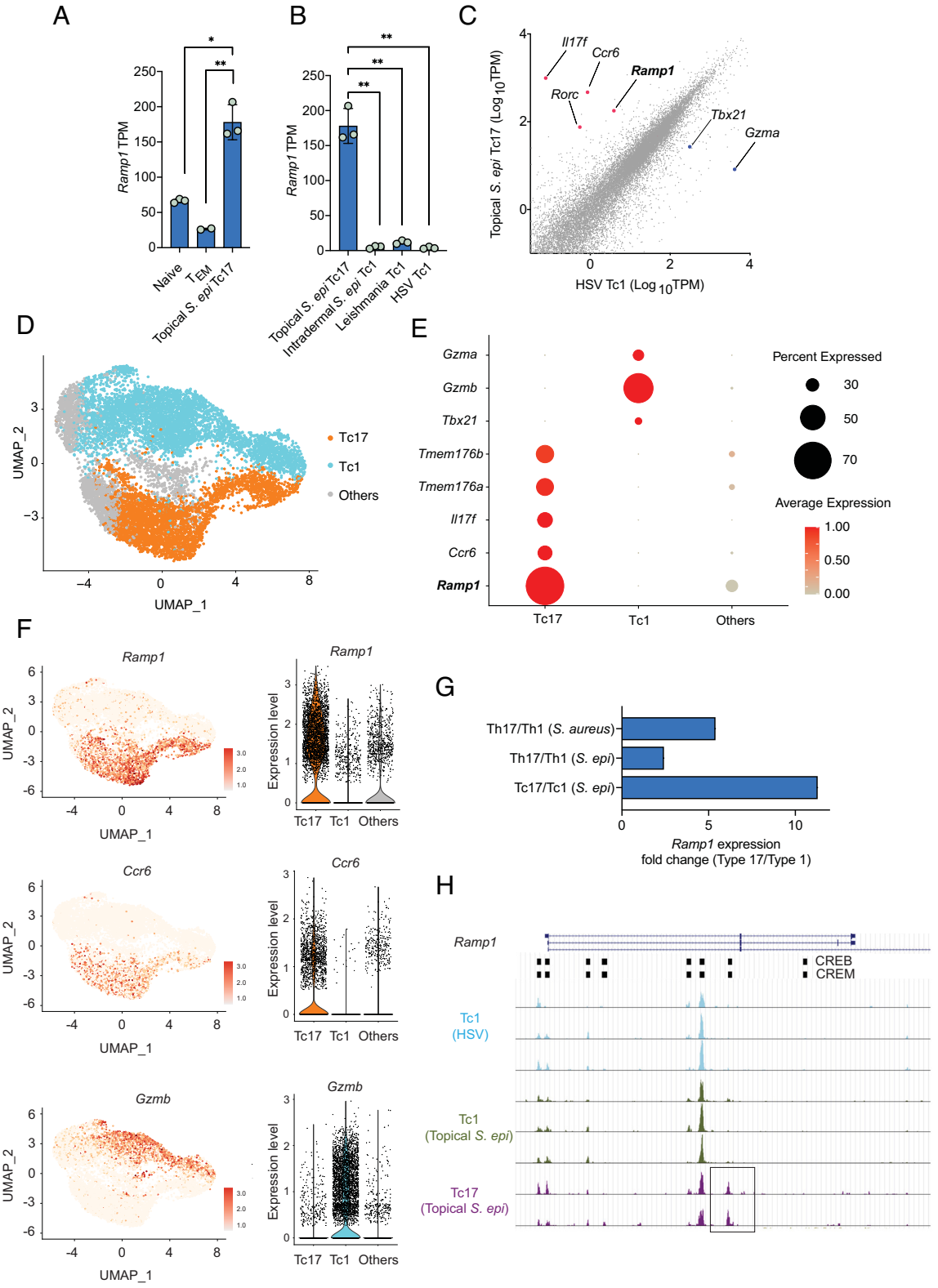

Fig. 2. Skin microbiota-reactive T cells express the receptor for the neuropeptide CGRP at homeostasis in vivo. (*A*) Comparison of *Ramp1* expression levels among the indicated T cell populations. "Naïve" refers to naïve T cells isolated from the skin-draining lymph nodes of *S. epidermidis*–associated animals. "T_{EM}" refers to effector memory T cells isolated from the skin-draining lymph nodes of *S. epidermidis*–associated animals. Tc17 refers to CCR6$^+$ CD8$^+$ T cells. (*B*) Comparison of *Ramp1* expression levels among the indicated T cell populations from the skin. (*C*) Scatter plot showing differentially expressed genes, comparing topical *S. epidermis*–induced Tc17 cells vs. HSV-induced Tc1 (CCR6$^-$ CD8$^+$) cells from the skin. Red and blue large dots highlight differentially expressed genes of interest. (*D*) Single-cell RNA-seq data of sorted skin CD8$^+$ T cells from animals topically associated with *S. epidermidis*. Clusters were assigned based on expression levels of canonical Tc1 and Tc17 markers, including those shown in (*E*). (*E*) Dot plot for scRNA-seq data, showing the frequency of each population of skin CD8$^+$ T cells expressing the indicated Tc1 or Tc17 markers and *Ramp1*, as well as the expression level for each transcript. Dots are colored by average expression and scaled by number of cells expressing the indicated transcript within each cluster (frequency). (*F*) Feature plots and violin plots for scRNA-seq data, showing the distribution and the frequency of each population of skin CD8$^+$ T cells expressing key transcripts indicated. (*G*) Comparison of expression of *Ramp1* in microbiota-induced Type 17 T cells vs. Type 1 T cells elicited by the indicated commensal colonization from RNA-seq datasets generated in our laboratory. (*H*) UCSC Genome Browser image of open chromatin regions of the *Ramp1* locus in the indicated CD8$^+$ T cell populations from the ATAC-seq dataset. Refer to detailed RNA-seq and ATAC-seq data sources and experimental settings in *Materials and Methods*. Bar graphs show mean ± SD. *P*-values were calculated with Student's *t* test. See also *SI Appendix*, Fig. S2.

or not detected in pathogenic CD8$^+$ T cells accumulating in the skin after *S. epidermidis* intradermal infection, Herpes simplex virus (HSV) infection or *Leishmania* infection (Fig. 2*B* and *SI Appendix*, Fig. S2*B*). Expression of another CGRP co-receptor encoding gene *Calcrl* remained low and undistinguishable across the skin T cell populations under diverse conditions (*SI Appendix*, Fig. S2*C*), suggesting that dynamic expression of *Ramp1* likely plays a dominant role in CGRP signaling in T cells, at least in the host-microbiota dialog in the skin compartment.

Ramp1 was significantly upregulated in commensal-induced Tc17 cells in comparison to another commensal-induced population, Tc1 cells (CCR6$^-$ CD8$^+$) (*SI Appendix*, Fig. S2*D*). Furthermore, the magnitude of *Ramp1* upregulation in commensal-induced Tc17 vs. *Ramp1^{low}* Tc1 cells was substantial, comparable to the induction of key Type 17 response genes such as *Ccr6, Il17f,* and *Rorc* in all Tc17 vs. Tc1 comparisons performed under different conditions (topical *S. epi* vs. HSV in Fig. 2*C*, topical vs. intradermal *S. epi* in *SI Appendix*, Fig. S2*B* and Tc17 vs. Tc1 in *SI Appendix*, Fig. S2*D*). Single-cell transcriptomic analysis of CD8$^+$ T cells isolated from the skin following *S. epidermidis* topical association [Fig. 2*D*, scRNA-seq dataset from our laboratory (30)] further corroborated that *Ramp1* upregulation was enriched in the Tc17 population (defined as the cluster with induction of Type 17 response genes including *Ccr6, Il17a, Il17f, Tmem176a, Tmem176b*), in contrast with the Tc1 population (defined as the cluster with induction of Type 1 response genes including *Tbx21, Gzma, Gzmb*) (Fig. 2 *E* and *F*).

Additionally, we observed upregulation of *Ramp1* in *S. epidermidis*–induced Type 17 CD4$^+$ T cells (Th17), which also accumulate in the skin after *S. epidermidis* topical colonization (28), compared to their *Ramp1^{low}* Th1 counterparts (*SI Appendix*, Fig. S2*E*) (37, 38). The magnitude of *Ramp1* upregulation in Th17 was comparable to key Type 17 response genes such as *Ccr6, Il17f,* and *Rorc* (*SI Appendix*, Fig. S2*E*). Furthermore, elevated expression of *Ramp1* was observed in Th17 cells accumulating in the skin after topical association with another skin commensal, *S. aureus* (32). Of note, mucosal-associated invariant T (MAIT) cells, which are imprinted by the microbiota (31), also exhibited upregulation of *Ramp1* in their CCR6$^+$/Type 17 subsets in various barrier compartments [*SI Appendix*, Fig. S2*F*, scRNA-seq dataset from our laboratory (31)]. Taken together, these observations illustrate that upregulation of the receptor for the neuropeptide CGRP, RAMP1, is a conserved attribute of diverse populations of Type 17 classical (Fig. 2*G*) and non-classical (*SI Appendix*, Fig. S2*F*) T cells and may contribute to neuroimmune crosstalk in response to a broad array of commensal microbes at barrier surfaces under homeostasis.

To further understand the mechanisms underlying upregulation of the neuroimmune CGRP–RAMP1 axis in commensal-induced T cells under steady state, we analyzed ATAC-seq (ATAC-sequencing) data, previously generated in our laboratory (30), performed in Tc1, Tc17, Th1, and Th17 cells accumulating in the skin following *S. epidermidis* topical association. Notably, we identified regions of accessible chromatin corresponding to regulatory elements of *Ramp1* that are unique to commensal-induced Tc17 and Th17 populations, compared to their Tc1 and Th1 counterparts (boxed regions in Fig. 2*H* and *SI Appendix*, Fig. S2*G*), consistent with transcriptional upregulation of *Ramp1*. Notably, these open chromatin regions of *Ramp1* enriched in Tc17 and Th17 cells contained cyclic adenosine monophosphate (cAMP)-responsive elements such as CREB and CREM motifs (Fig. 2*H*), pointing to potential engagement of Type 17 cell–specific *Ramp1* enhancers with cAMP and its transducers known to be downstream of CGRP signaling (39, 40). These observations may mechanistically account for transcriptional upregulation of *Ramp1* in commensal-induced skin Tc17 and Th17 populations at homeostasis, pointing to a role for CGRP signaling in reinforcing positive feedback on its own receptor expression via cAMP-dependent transcription factors that can bind to Type 17 cell–specific open chromatin regions of *Ramp1*.

Collectively, our observations unveiled a robust induction of the CGRP receptor RAMP1 specifically in Type 17 commensal-induced T cells, potentially endowing the T cells with an ability to communicate directly with the sensory nervous system in the skin under steady state.

Neuroimmune CGRP–RAMP1 Signaling Constrains Type 17 Responses in Commensal-Induced T Cells. To examine the extent to which CGRP–RAMP1 signaling in commensal-reactive T cells impacts lymphocyte functions, we genetically ablated *Ramp1* expression specifically in the T cells, utilizing a conditional knockout model, breeding *Ramp1 fl/fl* mice with *Lck Cre* mice. Because CGRP–RAMP1 signaling functions in many compartments in the skin including sensory nerves, the endothelium, and innate immune cells (40), a T cell–specific RAMP1 depletion approach is essential to unambiguously exclude any indirect or cell-nonautonomous impacts of CGRP on commensal-induced T cells at the barrier site.

To characterize the mechanisms underlying neuroimmune CGRP–RAMP1 signaling in commensal-induced T cells under steady state in an unbiased manner, we performed single-cell RNA-seq on CD8$^+$ T cells isolated from the skin of mice lacking *Ramp1* expression specifically in the T cell compartment (*Lck Cre+ Ramp1 fl/fl*) vs. control animals (*Lck Cre- Ramp1 fl/fl*), following *S. epidermidis* topical colonization (Fig. 3*A*) (37, 38). Consistent with the RNA-seq data described in Fig. 2, we observed upregulated *Ramp1* expression exclusively in the Tc17 populations, but not in the Tc1 or other populations (Fig. 3 *B*–*D*). Importantly, the *Ramp1* expression level in these Tc17 cells was significantly attenuated in the *Lck Cre+ Ramp1 fl/fl* genetic background compared to control (Fig. 3 *C* and *D*), confirming our robust T cell–specific *Ramp1* ablation approach. Of note, the number and the frequency of cells in each of the dominant Tc17 clusters (clusters 0 and 10) in the T cell–specific *Ramp1*-deficient genetic background were increased, compared to control (Fig. 3*E* and *SI Appendix*, Fig. S3*A*), indicating that RAMP1 may act to constrain accumulation and/or activation of commensal-induced Tc17 cells in the skin at homeostasis.

To determine whether the CGRP–RAMP1 axis modulates Type 17 responses in commensal-induced T cells, we examined the skin immune cells of animals lacking *Ramp1* in the T cell compartment vs. control animals by flow cytometry following *S. epidermidis* topical association. We found that RAMP1 deficiency in T cells significantly enhanced both the frequency and the cell number of the skin commensal–induced CD8$^+$ T cells that produced IL-17A and IL-17F, compared to control, under steady state in the skin (Fig. 3*F*). Consistent with RAMP1 functioning to restrain Type 17 responses in commensal-induced T cells, we observed an overall upregulation of key Type 17 mRNA transcripts in the T cell–specific *Ramp1*-deficient CD8$^+$ T cells, compared to wild-type control under steady state (*SI Appendix*, Fig. S3*B*). To determine whether the neuropeptide CGRP can regulate Type 17 cytokine production by T cells, we then utilized an ex vivo culture approach, assessing IL-17A production in sorted and cultured commensal-induced Tc17 and Th17 cells in the presence of different concentrations of CGRP with TCR stimulation via administration of anti-CD3e (Fig. 3*G*). Commensal-induced Tc17 and Th17 cells isolated from the skin exhibited diminished IL-17A production in response to CGRP in a dose-dependent manner ex vivo (Fig. 3*G* and *SI Appendix*, Fig. S3*E*). Taken together, these observations revealed a neuroimmune role of CGRP, demonstrating that T cell–intrinsic CGRP–RAMP1 signaling functions

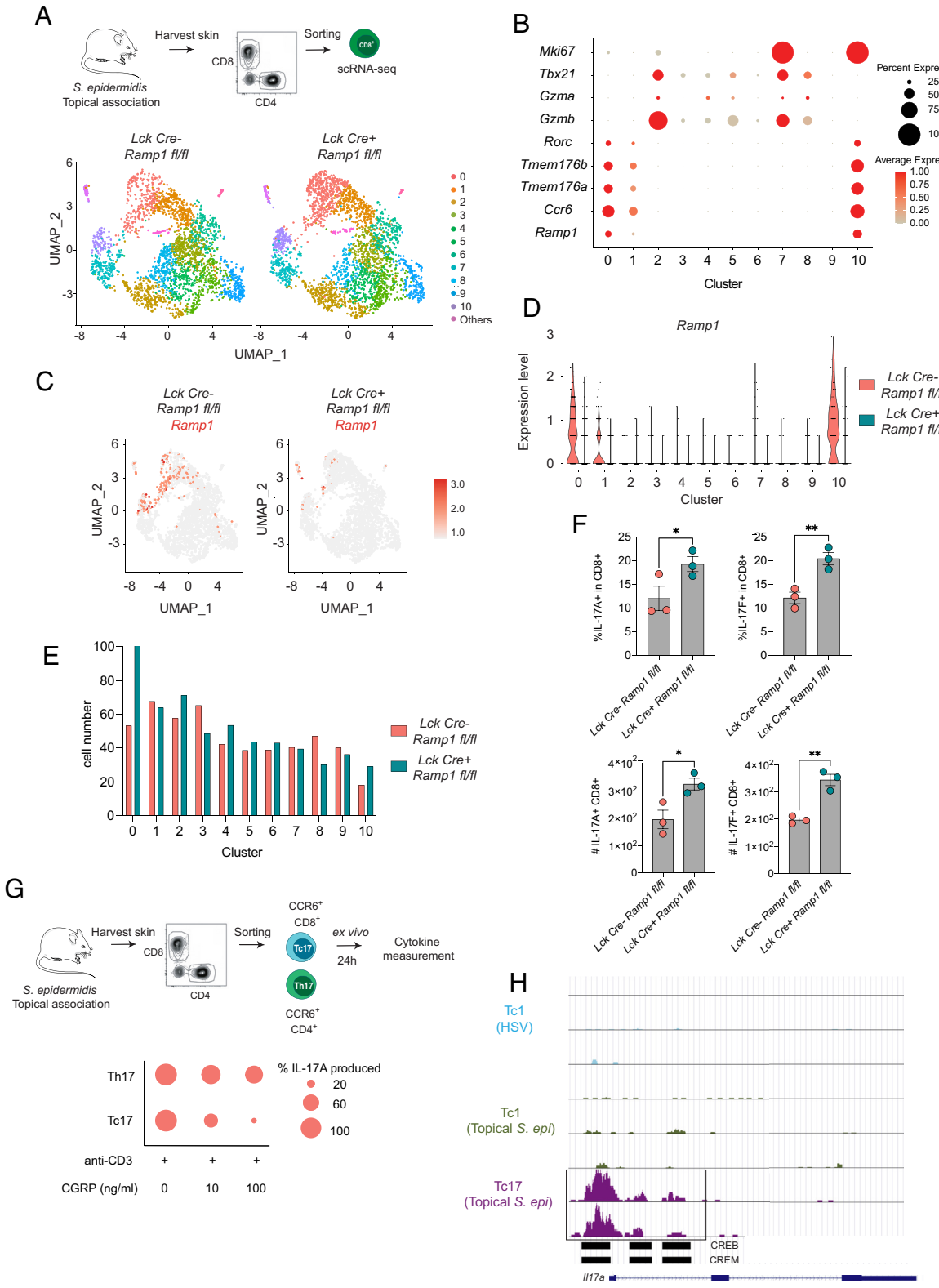

Fig. 3. The neuroimmune CGRP–RAMP1 axis constrains Type 17 responses in commensal-induced T cells in vivo. (*A*) Schematic for the scRNA-seq experimental workflow (*Top*). UMAP plots show all sorted CD8$^+$ T cells from *Ramp1*-deficient and control mice (*Bottom*). Assigned Seurat clusters are numbered and color-coded. (*B*) Dot plot showing the frequency of each population of skin CD8$^+$ T cells expressing the indicated Tc1 or Tc17 markers and *Ramp1*, as well as the expression level for each transcript, from both *Ramp1*-deficient and control mice combined. Dots are colored by average expression and scaled by number of cells expressing the indicated marker within each cluster (frequency). (*C*) UMAP plots showing *Ramp1* expression levels in all cells for each indicated genotype. (*D*) Violin plot showing expression of *Ramp1* for each Seurat cluster for each indicated genotype. (*E*) Bar graph representing the cell number from each genotype (*Ramp1*-deficient vs. control genetic background) for each assigned Seurat cluster. (*F*) Bar graphs illustrating flow cytometry data from each indicated genotype. Data represent two independent experiments. Bar graphs show mean ± SEM. *P*-values were calculated with Student's *t* test. (*G*) Dot plot (*Bottom*) showing the extent to which IL-17A was produced by Tc17 and Th17 cells isolated and treated ex vivo based on the schematic shown (*Top*). IL-17A production levels in the supernatants are reflected by the scaling of each dot in the plot. The "%IL-17A produced" value determining the scaling of each dot was calculated based on each IL-17A level normalized to control condition (without CGRP) from the same experiment. Cytokine measurement was performed using FlowCytomix bead array assay. Data represent two independent experiments. (*H*) UCSC Genome Browser image of open chromatin regions of the *Il17a* locus in the indicated CD8$^+$ T cell populations in the wild-type genetic background from the ATAC-seq data described in Fig. 2. See also *SI Appendix*, Fig. S3.

at the barrier site to constrain Type 17 responses in microbiota-induced T lymphocytes at homeostasis.

To gain further insights into how CGRP–RAMP1 signaling controls Type 17 T cell responses to the microbiota under steady state, we utilized our previously generated ATAC-seq (30). With this approach, we identified regions of open chromatin unique to Tc17 and Th17 cells in Type 17 response genes (boxed regions in Fig. 3*H* and *SI Appendix*, Fig. S3 *C* and *D*), in the wild-type genetic background. Importantly, we identified cAMP-responsive elements such as CREB and CREM motifs (boxed regions in Fig. 3*H* and *SI Appendix*, Fig. S3 *C* and *D*) in the Tc17/Th17-specific open chromatin regions of Type 17 response genes. Our motif identification suggests potential transcriptional regulation of Type 17 gene expression by cAMP and its transducers, downstream of neuroimmune CGRP–RAMP1 signaling, to constrain Type 17 responses in commensal-induced T cells in the skin at homeostasis.

Neuroimmune CGRP–RAMP1 Signaling Tunes T Cell Activation Status and Shapes Barrier Tissue Physiology. The impact of CGRP–RAMP1 signaling on Type 17 responses in T cells suggested that T cell behavior and activation status may also be subject to neuroimmune control in the skin. To address this point, we generated transgenic commensal-specific T lymphocytes (Bowie^{Tg}) that can be distinguished visually between wild-type (OFP^{+}) and *Ramp1*-deficient (GFP^{+}) upon adoptive transfer to a common host and tissue environment (Fig. 4*A*). Following *S. epidermidis* colonization, *Ramp1*-deficient Bowie^{Tg} T cells in the skin exhibited higher sphericity in their morphology over the intravital recording period compared to wild-type Bowie^{Tg} T cells (Fig. 4*A*), indicating that the T cells without CGRP–RAMP1 signaling may have heightened activation status, as high sphericity/rounding is associated with elevated calcium levels in T cells (36). Indeed, the enhanced sphericity in *Ramp1*-deficient Bowie^{Tg} T cells was reminiscent of rounding observed in the population of T cells that were distant from sensory fibers, as described in Fig. 1. Of note, *Ramp1*-deficient Bowie^{Tg} T cells overall exhibited a similar morphology pattern to the population of wild-type Bowie^{Tg} T cells that were distant from sensory nerve fibers (higher sphericity in vivo, Fig. 1*D*), pointing to a convergent state of heightened T cell activation/rounding that occurs when neuroimmune communication is disrupted or attenuated by either increased physical distances (Fig. 1*D*) or genetic ablation of *Ramp1* (Fig. 4*A*). Furthermore, the relationship between T cell morphology and physical association with sensory fibers in vivo was dominantly RAMP1-dependent (*SI Appendix*, Fig. S4*A*). Taken together, our intravital neuroimmune observations propose that the neuroimmune CGRP–RAMP1 axis modulates cellular morphology and behavior, potentially reflecting commensal-specific T cell activation status in the skin.

To assess whether T cell activation status was altered in the absence of CGRP–RAMP1 signaling, we compared transcriptomic profiles between wild-type and *Ramp1*-deficient commensal-induced T cells in our scRNA-seq dataset described in Fig. 3. Because *Ramp1* is expressed and acts mainly in Tc17 cells (Figs. 2 and 3), we focused on transcriptomic differences (*Lck Cre*- vs. *Lck Cre*+) in two dominant Tc17 populations—clusters 0 and 10, all with high baseline *Ramp1* expression in the *Cre*- control background vs. efficient *Ramp1* ablation in the *Cre*+ background. Of note, the most striking transcriptomic distinction between wild-type and *Ramp1*-deficient commensal-induced Tc17 cells was observed in the most abundant Tc17 cluster (cluster 0), where the differentially expressed genes exhibited highly significant enrichment in factors controlling T cell activation (Fig. 4*B*). Notably, in this dominant Tc17 cluster, we observed upregulation of genes encoding T cell activation markers TIM-3, PD-1 and CD44 in *Ramp1*-deficient T cells (*SI Appendix*, Fig. S5*A*), consistent with an overall increase in activation in Tc17 cells, as reflected in heightened Type 17 responses (Fig. 3), and altered cellular morphology (Fig. 4*A*). Another Tc17 cluster (cluster 10; *Mki67^{high}*) also harbored *Ramp1*-dependent differentially expressed genes, enriched in biological processes involving cell division, indicating that the CGRP–RAMP1 axis may also control proliferation in this actively dividing subset of Tc17 cells (*SI Appendix*, Fig. S5 *B* and *C*). Collectively, these observations point to a role of neuroimmune CGRP–RAMP1 signaling in regulating T cell activation status, specifically in commensal-induced Tc17 cells at the barrier site at homeostasis.

To assess the functional significance of neuroimmune-mediated constraint of microbiota-reactive T cells in the skin, we asked whether heightened activity of *Ramp1*-deficient T cells may impact the broader activation status and physiology of the skin.

To this end, we focused on keratinocytes, which play a major role in maintaining cutaneous tissue integrity in the host-microbiota dialog (28). Specifically, we compared the transcriptional profiles of keratinocytes in the tissue environment where bystander commensal-reactive T cells were either *Ramp1*-deficient (*Lck Cre+ Ramp1 fl/fl*) or wild-type control (*Lck Cre– Ramp1 fl/fl*) (37, 38). Of note, our transcriptomic analysis showed that keratinocytes did not express *Ramp1*, and therefore any alterations in the keratinocyte transcriptomes would be attributed to cell-nonautonomous sources such as differential *Ramp1* expression levels in the T cell compartment. We observed that keratinocytes in the milieu with *Ramp1*-deficient commensal-induced T cells exhibited upregulation of genes associated with ectopic tissue activation, such as those involved in histone modification, nucleosome organization, electron transport chain, and protein translation (Fig. 4*C*), corresponding to the heightened activation status of bystander *Ramp1*-deficient T cells under steady state. Furthermore, we also observed upregulation of defined retroelements and non-coding transcripts in keratinocytes from animals with *Ramp1*-deficient commensal-induced T cells (Fig. 4*D* and *SI Appendix*, Fig. S5*D*), which have been associated with increased immune response or inflammation in defined settings (41).

To further assess whether the control of Type 17 responses and keratinocyte activation status by neuroimmune CGRP–RAMP1 signaling can confer functional consequences on the barrier tissue in vivo, we assessed epithelial wound repair, which we had previously shown to be linked to commensal-induced T cells and Type 17 responses in the skin (29, 42). We observed that the lack of neuroimmune CGRP–RAMP1 signaling axis in commensal-induced T cells resulted in enhanced wound healing upon injury (Fig. 4*E*, also confirmed with an independent activated T cell–specific *Ox40 Cre* system), in accordance with the heightened Type 17 responses in *Ramp1*-deficient T cells. The impact of the CGRP–RAMP1 axis on tissue repair demonstrates that alterations in neuroimmune signaling in commensal-induced T cells enhance Type 17 responses and the overall activation status of keratinocytes, thereby shaping the outcome of biological processes governing tissue health and integrity.

Taken together, our observations illustrate that neuroimmune CGRP–RAMP1 signaling in microbiota-reactive T lymphocytes constrains Type 17 response and controls T cell activation, shaping the tissue milieu and profoundly impacting the activation status of the epithelial compartment (Fig. 4*F*), which can have vast implications on tissue physiology particularly under additional insults or pathology.

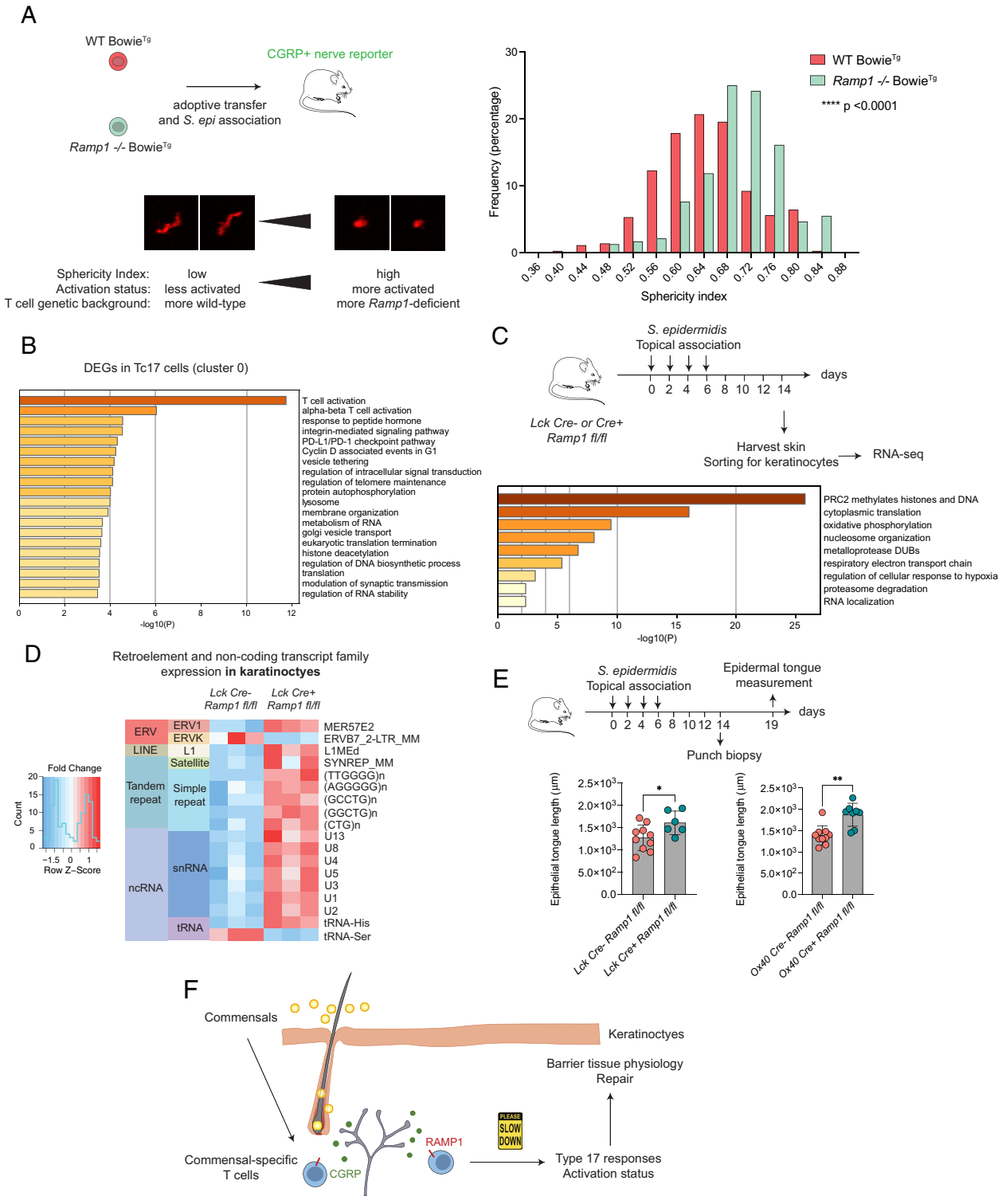

Fig. 4. Neuroimmune CGRP–RAMP1-mediated regulation of microbiota-reactive T cells shapes barrier tissue physiology. (*A*) The *Top* schematic depicts the experimental setup where commensal-specific (Bowie^{Tg}) T cells from *Ramp1*-deficient and control genetic backgrounds, expressing distinct fluorophores, were adoptively transferred to common hosts harboring the *Calca-EGFP* reporter for sensory fiber visualization, followed by *S. epidermidis* topical association. The graph represents distribution of cellular sphericity values over the recording period for each indicated genotype of the commensal-specific T cells. Statistical significance was determined using all sphericity index values over the defined recording period, comparing the WT Bowie^{Tg} population vs. the *Ramp1*-deficient Bowie^{Tg} population. *P*-values were calculated with Student's *t* test. The *Bottom* schematic shows representative images of the cells with the indicated range of sphericity values and summarizes the relationship between cell shape/potential activation status and *Ramp1* genetic background. Data represent two independent experiments. (*B*) GO enrichment analysis of differentially expressed genes in the dominant, non-proliferating Tc17 cluster (Cluster 0 from the scRNA-seq dataset described in Fig. 3), comparing commensal-induced T cells from *Ramp1*-deficient vs. control genetic backgrounds. (*C*) GO enrichment analysis of differentially expressed genes, comparing keratinocytes from the skin milieu where commensal-induced T cells were *Ramp1*-deficient vs. control. (*D*) Analysis of families of differentially expressed retroelement and non-coding transcript loci, comparing keratinocytes from the skin milieu where commensal-induced T cells were *Ramp1*-deficient vs. control. (*E*) Quantification of the epidermal tongue length 5 d after wounding in male animals from the indicated genotypes, following *S. epidermidis* topical association (full body). Bar graphs show mean ± SD. *P*-values were calculated with Student's *t* test. Data represent three independent experiments. (*F*) A schematic summarizing the neuroimmune CGRP–RAMP1 axis functioning to constrain commensal-induced T cells and regulate barrier tissue physiology. See also *SI Appendix*, Figs. S4 and S5.

Discussion

In this study, we have established and delineated the physical and functional interface between the sensory nervous system and adaptive immunity to the microbiota at the largest barrier tissue at homeostasis. First, we demonstrated close physical proximity between commensal-specific T lymphocytes and cutaneous nerve peripherals. We then identified a key neuropeptide and its receptor (CGRP–RAMP1) as a signaling mechanism mediating the direct communication between local neural fibers and microbiota-reactive T cells in the skin. We then proceeded to elucidate the mechanisms by which the neuroimmune CGRP–RAMP1 signaling axis modulated Type 17 responses and shaped the transcriptome and activation status of commensal-induced Type 17 T cells under steady state, contributing to remodeling of the barrier site milieu. Collectively, these observations unveil a role of CGRP as a physiological neuroimmune signaling molecule that can impact adaptive immunity and subsequently the skin tissue environment and barrier integrity.

Previous studies have established neuroimmune communication in the context of innate immunity under infection or tissue inflammation in diverse barrier tissues in mammals (2), as well as in invertebrate model organisms of host-microbe interactions (43, 44). Our study has further identified a neuroimmune regulation mechanism in which adaptive lymphocytes can directly respond to neuronal signals under steady state, in the absence of pathogens or pro-inflammatory cues. Specifically, under homeostasis, commensal-specific T cells, which are highly plastic and can promote antimicrobial defense and repair, are capable of directly communicating with sensory fibers via CGRP. The ability of these lymphocytes to respond to constantly fluctuating sensory signals relayed to them by sensory neurons via CGRP is another testament to multisystem coordination and adaptability that the host has evolved to maintain barrier site homeostasis, particularly in the context of a complex host-microbiota dialog. Indeed, commensal-reactive T cells expressed additional neuropeptide, neurotrophin, or neuroendocrine signaling-related genes in addition to those involved in the CGRP–RAMP1 signaling axis, indicating that there are a variety of neuroimmune signal transduction pathways beyond CGRP–RAMP1 to tune adaptive immunity to the microbiota. Of note, catecholamines and adrenergic signaling have been shown to regulate $CD8^+$ T cell effector functions in the context of viral infection and anti-tumor therapy (45). Notably, sensory neurons express chemokines (46), and therefore chemokine receptors often found expressed in T cells present yet another neuroimmune communication mechanism in parallel to the CGRP–RAMP1 axis. Collectively, these diverse neuroimmune molecules expressed at the T cell–nerve interface highlight a dynamic and multipronged dialog between the immune system and the sensory nervous system. Of note, sensory neurons have been shown to exert multimodal control on another immune compartment, dendritic cells, via diverse mechanisms of neuroimmune regulation involving neuropeptides, chemokines including CCL2 and electrical activity (47).

Our study has further corroborated the remarkably pleiotropic and context-dependent effects of CGRP on diverse immune compartments across barrier tissues. In the skin, while sustained or potent activation of sensory neurons has been demonstrated to elicit 1) an anticipatory protective immune response in the context of fungal infection and optogenetic stimulation (14, 25) or 2) an anti-inflammatory response to bacterial pathogens (13, 15), we propose that short-term or tonic releases of CGRP from sensory fibers in our setting of homeostatic host-microbiota interaction may moderate or constrain the adaptive immune response in the skin, possibly to circumvent collateral tissue damage or excessive metabolic cost. The precise molecular mechanisms underlying how CGRP remodels the transcriptome and proteome of commensal-reactive T cells, which may in part involve protein kinase A /cAMP response element-mediated signaling pathways, reminiscent of previous findings in the context of CGRP-dependent anti-inflammatory responses in dendritic cells and macrophages (39, 48, 49), remain to be studied. Furthermore, CGRP may be able to modulate the immune system indirectly by reshaping the skin microbiota, potentially via a similar mechanism where substance P regulates the composition of the microbiota in the gut to promote tissue protection (50).

Sources of physiological sensory modalities that can modify commensal-specific T cell activity and the tissue milieu may include temperature, noxious pain, mechanical stimuli, microbially derived molecules, as well as direct or indirect consequences of diets, skincare products, pain management, or cancer treatment. Direct perturbations of systemic CGRP activity such as migraine treatment or prevention (51, 52) may also be able to impact commensal-specific lymphocytes at the barrier tissue, potentially contributing to side effects over the course of this powerful migraine therapeutic or prophylactic approach. Intriguingly, many side effects from migraine management that have been documented, such as exacerbated inflammation (10), altered course of wound healing or bruising (53, 54) and alopecia (55), involved dysregulation at barrier tissues, raising an intriguing possibility that intervention with the CGRP–RAMP1 axis may have broader consequences at barrier sites in the clinical or human health context. With the emergence of acute migraine treatment approaches such as intranasal sprays (56), where CGRP modulatory molecules are directly deposited at barrier tissues such as the nasal mucosa, the uncharacterized impact of CGRP on local tissue physiology, whether adverse or beneficial to human health, warrants further studies.

The neuroimmune CGRP–RAMP1 signaling axis has been shown to influence lymphoid developmental stages beyond antigen-experienced T cells in the adult skin. Specifically, CGRP–RAMP1 promotes hematopoiesis and hematopoietic stem cell mobilization (57, 58), as well as thymocyte education (59). Our characterization and re-contextualization of CGRP–RAMP1 signaling in commensal-induced T cells in the skin at homeostasis may reinforce the idea that the CGRP–RAMP1 axis is a temporally and spatially versatile rheostat of lymphocyte activity, rapidly tuning its activity to sensory modalities, particularly in commensal-specific T cells that are extremely plastic and are situated in the environment that constantly encounters changing physical and microbial cues. Because adaptive immune cell activation is already highly antigen-specific and antigen-dependent, CGRP may not directly mediate or modulate the antigen recognition steps. On the contrary, because the innate immune arm lacks specific antigen recognition, the input from the nervous system, such as CGRP, neuromedin, and catecholamines, may play a more prominent role as a licensing agonist or an immunoregulatory factor in innate and innate-like immune cells (60–62). We propose that CGRP participates in functional fine-tuning of commensal-specific adaptive immunity, which may have implications in shaping the dynamic interactions between innate and adaptive immune compartments.

It is notable that only the subset of adaptive lymphocytes involved in Type 17 responses, but not those mediating Type 1 responses, has evolved a CGRP–RAMP1-dependent mechanism to communicate directly with the sensory nervous system. Because Type 17 responses are associated with extracellular microbes and epithelial surfaces, we speculate that Tc17 and Th17 cells have evolved the ability to engage not only with antigens but also with

neuronal signals, both of which are enriched in the highly innervated skin. Barrier surface cues such as abiotic (temperature, noxious pain) and microbially derived (pathogen- or damage-associated molecular patterns) stimuli can directly activate sensory fibers (63) and trigger CGRP release. CGRP-mediated neuroimmune tuning may then allow *Ramp1*-expressing Type 17 commensal-specific T cells to respond more effectively to fluctuating cues at these epithelial surfaces. Of note, in the context of autoimmunity and inflammation, cAMP-responsive elements downstream of the CGRP–RAMP1 axis have been shown to be involved in Th17 differentiation (64, 65). Furthermore, ILC3s, which regulate barrier integrity and defense through IL-17 and IL-22, are under the control of the VIP neuropeptide released from feeding-dependent enteric neurons (66–68), as well as neuromodulators produced by enteric glial cells (69), pointing to a paramount role of neuroimmune coordination in maintaining organ function and promoting barrier protection. Intriguingly, intestinal goblet cells, which play instrumental roles in maintaining barrier integrity, also respond to CGRP via RAMP1 to promote mucus production (70), illustrating another instance where sentinel cells at the epithelial surface are subject to regulation by this critical neuropeptide, which appears to mediate a wide range of multisystem crosstalk at barrier tissues. Additionally, in light of the expression of *Ramp1* in Type 17 unconventional T cells at homeostasis (*SI Appendix*, Fig. S2*F*), we speculate that defined populations of microbiota-imprinted MAIT and potentially γδ T cells in the naïve mouse skin may also be subject to CGRP-mediated neuronal control, the functional consequences of which remain to be studied.

Tuning of commensal-induced T cells by the neuroimmune CGRP–RAMP1 axis can functionally impact barrier tissues, as we showed that *Ramp1*-deficient T cells, refractory to the local neuronal signal and behaving in a manner that is less restrained in Type 17 immunity and activation status, were able to promote tissue repair or result in ectopic activation of keratinocytes. Whether enhanced epithelial activation and wound repair resulting from *Ramp1*-deficient T cells are dependent on Type 17 cytokines remains to be determined. Because of the direct role of IL-17A in expediting epithelial healing (42) and skin sensory nerve repair (32), we speculate that IL-17 may be a dominant mediator of neuroimmune control of microbiota-reactive T cells and wound repair, though it is plausible that other T cell–associated molecules that are regulated by CGRP may also contribute to this phenomenon. Because sustained, unfettered activation of T cells and concomitant hyperactivation of the epithelial tissue milieu may trigger collateral tissue damage, particularly in immunopathological settings, we propose that homeostatic CGRP–RAMP1-dependent tuning of commensal-reactive lymphocytes may serve as both a guardrail and a rheostat of adaptive immunity to moderate barrier tissue physiology, in the presence of ever-changing cues or potential threats from microbes and sensory modalities. In light of the ability of CGRP–RAMP1 signaling to modulate anti-tumor immunity mediated by $CD8^+$ T cells (71), we anticipate that better understanding of how the neuroimmune CGRP–RAMP1 axis impacts homeostatic Type 17 adaptive immunity may contribute to a tailored and rationalized approach to reprogram or customize T cells in various clinical settings, via harnessing neuromodulators to suppress or enhance adaptive immunity at the microbiota-colonized barrier surfaces in the appropriate context of human health and immunopathology.

Materials and Methods

Mice. All mice were bred and maintained under specific pathogen-free (SPF) conditions at an American Association for the Accreditation of Laboratory Animal Care-accredited animal facility at NIAID and housed in accordance with the procedures outlined in the Guide for the Care and Use of Laboratory Animals. All experiments were performed under the animal study proposal LHIM-3E approved by the NIAID Animal Care and Use Committee. Unless otherwise noted, sex- and age-matched animals between 6 and 12 wk of age were used for each experiment. Refer to *SI Appendix, Supporting Text* for mouse strains.

Commensal Bacterial Culture and Colonization. Topical association with *S. epidermidis* NIHLM087 was performed as described in ref. 28. Refer to *SI Appendix, Supporting Text* for further details.

Murine Tissue Processing. To obtain skin single-cell suspensions, ear pinnae were excised and separated into dorsal and ventral sheets, and then placed in the digestion media described in *SI Appendix, Supporting Text*. Refer to *SI Appendix, Supporting Text* for detailed descriptions of T cell in vitro restimulation prior to flow cytometry.

Flow Cytometry. Murine single-cell suspensions were incubated with fluorochrome-conjugated antibodies against surface markers and intracellular markers listed in *SI Appendix*, Table S1. Refer to *SI Appendix, Supporting Text* for detailed descriptions of staining and data acquisition procedures.

Ex Vivo Culture and Cytokine Production Assessment. The indicated $CD4^+$ and $CD8^+$ T cell populations from the skin of commensal-colonized animals were isolated by fluorescence-activated cell sorting and cultured in the presence of TCR stimulation (1 μg/mL plate-bound anti-CD3e mAb, clone 145-2C11). Rat CGRP (α isoform; Sigma-Aldrich) at the indicated concentrations was added to the culture, and supernatants were collected 24 h later and subjected to the FlowCytomix bead array assay (eBioscience) for cytokine production assessment. Refer to *SI Appendix, Supporting Text* for further details.

Confocal Microscopy. Tissue whole-mount preparation and visualization were performed as described in ref. 31. Refer to *SI Appendix, Supporting Text* for detailed descriptions.

Intravital Microscopy and Analyses. An albino version of the *Calca-EGFP* reporter was generated by breeding albino B6 animals with *Calca-EGFP* animals. Albino mice heterozygous for *Calca-EGFP* were used for intravital imaging after an adoptive transfer with fluorochrome-expressing $Bowie^{Tg}$ cells (approximately 5×10^5 cells), followed by the same course of topical association with *S. epidermidis* (NIHLM087) described above. Intravital imaging was done 8 to 12 d after the initial commensal colonization to ensure optimal accumulation of fluorochrome-expressing $Bowie^{Tg}$ cells in the ear skin for visualization.

Intravital imaging and analyses were performed as described in ref. 32. Refer to *SI Appendix, Supporting Text* for detailed descriptions.

Single-Cell RNA-seq and Analysis. Skin $CD8^+$ lymphocytes labeled with TotalSeqC hashtag antibodies (BioLegend) from *S. epidermidis*–associated mice (six *Lck-Cre- Ramp1 fl/fl* animals and six *Lck Cre+ Ramp1 fl/fl* animals) were sorted as DAPI- $CD90.2^+$ $TCR\beta^+$ $CD4^-$ $CD8\beta^+$ $TCR\gamma\delta^-$ $CD49f^-$ $NK1.1^-$ $B220^-$ $CD11b^-$ $CD11c^-$ $MHCII^-$, using a Sony MA900 cell sorter. All samples were pooled together, and approximately 15,000 sorted cells were loaded onto the Chromium Single Cell Controller (10× Genomics) to encapsulate cells into droplets. The library was prepared using a Chromium Single Cell 5′ Reagent Kits v2 (10× Genomics) following the manufacturer's instructions, and then sequenced on an Illumina Nextseq500 (Next Seq 500/550 High Output Kit v2, Illumina).

Refer to *SI Appendix, Supporting Text* for further descriptions of analyses of the dataset (37, 38) and other publicly available scRNA-seq datasets, previously generated in our laboratory.

Bulk RNA-seq and Analysis. $CD4^+$ T cells from wild-type animals following *S. epidermidis* colonization were sorted into Th1 and Th17, processed, and analyzed for RNA-seq (37, 38) as described in ref. 29.

Keratinocytes from the same *Lck-Cre Ramp1 fl/fl* experiment described above were sorted and processed for RNA-seq as described in ref. 41. Sequencing reads were mapped to the mm10 (GRCm38) mouse genome using STAR with stringent mapping conditions, where reads aligned to multiple regions of the genome were eliminated (-outFilterMultimapNmax 2). Differential gene expression was calculated using HOMER's getDiffExpression (72). Genes with FDR < 0.05

and foldchange >2 were considered differentially expressed transcripts. Gene Ontology (GO) enrichment analysis for differentially expressed genes was performed using Metascape (73). Retroelement and noncoding transcript expression was determined using HOMER 4.11 (72), defining these transcripts based on the annotations provided by the Genome-based Endogenous Viral Element Database for GRCm38.

Refer to *SI Appendix, Supporting Text* for further descriptions of analyses of the dataset (37, 38) and other publicly available RNA-seq datasets, previously generated in our laboratory.

ATAC-seq. A publicly available ATAC-seq dataset, previously generated in our laboratory, from sorted $CD4^+$ and $CD8^+$ T cells under various conditions from ref. 30 was used for analyses in Figs. 2*H* and 3*H* and *SI Appendix*, Figs. S2*G* and S3 *C* and *D*. The dataset is available on NCBI BioProject PRJNA486019.

To scan for motif occurrences, HOMER's scanMoifGenomeWide.pl was used (72). The results were visualized in the UCSC Genome Browser (74) by uploading custom hubs.

Wounding and Epifluorescence Microscopy of Wound Tissue. Wounding and epifluorescence microscopy were performed as described in ref. 29. Refer to *SI Appendix, Supporting Text* for detailed descriptions.

Statistical Analysis. Prism 9 (GraphPad) was used to determine the indicated statistical significance.

Data, Materials, and Software Availability. RNA-seq data were deposited in the GEO database under accession GSE253041 (bulk RNA-seq) (37) and GSE253063 (single-cell RNA-seq) (38). Previously published data were used for this work (Select raw sequencing data previously generated in our laboratory were subjected to new analyses and described in the text, Figure Legends and *Materials and Methods*). All other data are included in the manuscript and/or supporting information.

ACKNOWLEDGMENTS. W.K. was supported by the Damon Runyon Cancer Research Foundation. Y.B. was supported by the Division of Intramural Research of the National Institute of Allergy and Infectious Diseases (1ZIA-AI001115 and 1ZIA-AI001132). We thank Dr. Margery Smelkinson, Galina Koroleva, Dr. Alexander T. Chesler, Dr. Seong-Ji Han, Kimberly Beacht, Ejae Lewis, Dr. Juliana Perez-Chaparro and Brittany Dulek for technical support, advice, and assistance with experiments. We thank Dr. Dorian McGavern, Dr. John O'Shea, and Dr. Wade Kingery for generously sharing the indicated mouse lines. We thank members of the Belkaid lab for technical input and assistance, as well as constructive feedback throughout the research project.

Author affiliations: [a]Metaorganism Immunity Section, Laboratory of Host Immunity and Microbiome, National Institute of Allergy and Infectious Diseases, NIH, Bethesda, MD 20892; [b]National Institute of Allergy and Infectious Diseases Microbiome Program, National Institute of Allergy and Infectious Diseases, NIH, Bethesda, MD 20892; [c]Biological Imaging Section, Research Technology Branch, National Institute of Allergy and Infectious Diseases, NIH, Bethesda, MD 20892; [d]Kimberly and Eric J. Waldman Department of Dermatology, Mark Lebwohl Center for Neuroinflammation and Sensation, Marc and Jennifer Lipschultz Precision Immunology Institute, and Friedman Brain Institute, Icahn School of Medicine at Mount Sinai, New York, NY 10029; [e]Department of Immunology, Harvard Medical School, Boston, MA 02115; and [f]Unite Metaorganisme, Immunology Department, Pasteur Institute, 75015 Paris, France

1. S. Talbot, S. L. Foster, C. J. Woolf, Neuroimmunity: Physiology and pathology. *Annu. Rev. Immunol.* **34**, 421–447 (2016).
2. C. Chu, D. Artis, I. M. Chiu, Neuro-immune interactions in the tissues. *Immunity* **52**, 464–474 (2020).
3. J. R. Huh, H. Veiga-Fernandes, Neuroimmune circuits in inter-organ communication. *Nat. Rev. Immunol.* **20**, 217–228 (2020).
4. J. Ordovas-Montanes *et al.*, The regulation of immunological processes by peripheral neurons in homeostasis and disease. *Trends Immunol.* **36**, 578–604 (2015).
5. H. Veiga-Fernandes, D. Mucida, Neuro-immune interactions at barrier surfaces. *Cell* **165**, 801–811 (2016).
6. R. G. J. Klein Wolterink, G. S. Wu, I. M. Chiu, H. Veiga-Fernandes, Neuroimmune interactions in peripheral organs. *Annu. Rev. Neurosci.* **45**, 339–360 (2022).
7. B. Becher, S. Spath, J. Goverman, Cytokine networks in neuroinflammation. *Nat. Rev. Immunol.* **17**, 49–59 (2017).
8. J. W. Kinney *et al.*, Inflammation as a central mechanism in Alzheimer's disease. *Alzheimers Dement. (N. Y.)* **4**, 575–590 (2018).
9. M. Charabati, M. A. Wheeler, H. L. Weiner, F. J. Quintana, Multiple sclerosis: Neuroimmune crosstalk and therapeutic targeting. *Cell* **186**, 1309–1327 (2023).
10. K. J. Tracey, The inflammatory reflex. *Nature* **420**, 853–859 (2002).
11. F. Matheis *et al.*, Adrenergic signaling in muscularis macrophages limits infection-induced neuronal loss. *Cell* **180**, 64–78.e16 (2020).
12. C. E. Le Pichon, A. T. Chesler, The functional and anatomical dissection of somatosensory subpopulations using mouse genetics. *Front. Neuroanat.* **8**, 21 (2014).
13. I. M. Chiu *et al.*, Bacteria activate sensory neurons that modulate pain and inflammation. *Nature* **501**, 52–57 (2013).
14. S. W. Kashem *et al.*, Nociceptive sensory fibers drive interleukin-23 production from CD301b+ dermal dendritic cells and drive protective cutaneous immunity. *Immunity* **43**, 515–526 (2015).
15. F. A. Pinho-Ribeiro *et al.*, Blocking neuronal signaling to immune cells treats streptococcal invasive infection. *Cell* **173**, 1083–1097.e22 (2018).
16. N. Y. Lai *et al.*, Gut-innervating nociceptor neurons regulate Peyer's patch microfold cells and SFB levels to mediate salmonella host defense. *Cell* **180**, 33–49.e22 (2020).
17. L. Riol-Blanco *et al.*, Nociceptive sensory neurons drive interleukin-23-mediated psoriasiform skin inflammation. *Nature* **510**, 157–161 (2014).
18. S. Zhang *et al.*, Nonpeptidergic neurons suppress mast cells via glutamate to maintain skin homeostasis. *Cell* **184**, 2151–2166.e16 (2021).
19. V. N. Lagomarsino, A. D. Kostic, I. M. Chiu, Mechanisms of microbial-neuronal interactions in pain and nociception. *Neurobiol. Pain* **9**, 100056 (2021).
20. A. Wallrapp *et al.*, Calcitonin gene-related peptide negatively regulates alarmin-driven type 2 innate lymphoid cell responses. *Immunity* **51**, 709–723.e6 (2019).
21. H. Xu *et al.*, Transcriptional atlas of intestinal immune cells reveals that neuropeptide alpha-CGRP modulates group 2 innate lymphoid cell responses. *Immunity* **51**, 696–708.e9 (2019).
22. H. Nagashima *et al.*, Neuropeptide CGRP limits group 2 innate lymphoid cell responses and constrains type 2 inflammation. *Immunity* **51**, 682–695.e6 (2019).
23. N. Serhan *et al.*, House dust mites activate nociceptor-mast cell clusters to drive type 2 skin inflammation. *Nat. Immunol.* **20**, 1435–1443 (2019).
24. C. Perner *et al.*, Substance P release by sensory neurons triggers dendritic cell migration and initiates the type-2 immune response to allergens. *Immunity* **53**, 1063–1077.e7 (2020).
25. J. A. Cohen *et al.*, Cutaneous TRPV1(+) neurons trigger protective innate type 17 anticipatory immunity. *Cell* **178**, 919–932.e14 (2019).
26. K. Honda, D. R. Littman, The microbiota in adaptive immune homeostasis and disease. *Nature* **535**, 75–84 (2016).
27. E. Ansaldo, T. K. Farley, Y. Belkaid, Control of immunity by the microbiota. *Annu. Rev. Immunol.* **39**, 449–479 (2021).
28. S. Naik *et al.*, Commensal-dendritic-cell interaction specifies a unique protective skin immune signature. *Nature* **520**, 104–108 (2015).
29. J. L. Linehan *et al.*, Non-classical immunity controls microbiota impact on skin immunity and tissue repair. *Cell* **172**, 784–796.e18 (2018).
30. O. J. Harrison *et al.*, Commensal-specific T cell plasticity promotes rapid tissue adaptation to injury. *Science* **363**, eaat6280 (2019).
31. M. G. Constantinides *et al.*, MAIT cells are imprinted by the microbiota in early life and promote tissue repair. *Science* **366**, eaax6624 (2019).
32. M. Enamorado *et al.*, Immunity to the microbiota promotes sensory neuron regeneration. *Cell* **186**, 607–620.e17 (2023).
33. S. Naik *et al.*, Compartmentalized control of skin immunity by resident commensals. *Science* **337**, 1115–1119 (2012).
34. E. S. McCoy, B. Taylor-Blake, M. J. Zylka, CGRPalpha-expressing sensory neurons respond to stimuli that evoke sensations of pain and itch. *PLoS One* **7**, e36355 (2012).
35. H. D. Moreau *et al.*, Signal strength regulates antigen-mediated T-cell deceleration by distinct mechanisms to promote local exploration or arrest. *Proc. Natl. Acad. Sci. U.S.A.* **112**, 12151–12156 (2015).
36. P. A. Negulescu, T. B. Krasieva, A. Khan, H. H. Kerschbaum, M. D. Cahalan, Polarity of T cell shape, motility, and sensitivity to antigen. *Immunity* **4**, 421–430 (1996).
37. Kulalert *et al.*, Sequencing data for "The neuroimmune CGRP–RAMP1 axis tunes cutaneous adaptive immunity to the microbiota." Gene Expression Omnibus (GEO). https://www.ncbi.nlm.nih.gov/geo/query/acc.cgi?acc=GSE253041. Deposited 12 January 2024.
38. Kulalert *et al.*, Sequencing data for "The neuroimmune CGRP–RAMP1 axis tunes cutaneous adaptive immunity to the microbiota." Gene Expression Omnibus (GEO). https://www.ncbi.nlm.nih.gov/geo/query/acc.cgi?acc=GSE253063. Deposited 12 January 2024.
39. M. D. Harzenetter *et al.*, Negative regulation of TLR responses by the neuropeptide CGRP is mediated by the transcriptional repressor ICER. *J. Immunol.* **179**, 607–615 (2007).
40. F. A. Russell, R. King, S. J. Smillie, X. Kodji, S. D. Brain, Calcitonin gene-related peptide: Physiology and pathophysiology. *Physiol. Rev.* **94**, 1099–1142 (2014).
41. D. S. Lima-Junior *et al.*, Endogenous retroviruses promote homeostatic and inflammatory responses to the microbiota. *Cell* **184**, 3794–3811.e19 (2021).
42. P. Konieczny *et al.*, Interleukin-17 governs hypoxic adaptation of injured epithelium. *Science* **377**, eabg9302 (2022).
43. K. Makhijani *et al.*, Regulation of Drosophila hematopoietic sites by Activin-beta from active sensory neurons. *Nat. Commun.* **8**, 15990 (2017).
44. D. H. Kim, S. W. Flavell, Host-microbe interactions and the behavior of Caenorhabditis elegans. *J. Neurogenet.* **34**, 500–509 (2020).
45. A. M. Globig *et al.*, The beta(1)-adrenergic receptor links sympathetic nerves to T cell exhaustion. *Nature* **622**, 383–392 (2023).
46. I. M. Chiu *et al.*, Transcriptional profiling at whole population and single cell levels reveals somatosensory neuron molecular diversity. *Elife* **3**, e04660 (2014).
47. P. Hanc *et al.*, Multimodal control of dendritic cell functions by nociceptors. *Science* **379**, eabm5658 (2023).
48. F. Altmayr, G. Jusek, B. Holzmann, The neuropeptide calcitonin gene-related peptide causes repression of tumor necrosis factor-alpha transcription and suppression of ATF-2 promoter recruitment in toll-like receptor-stimulated dendritic cells. *J. Biol. Chem.* **285**, 3525–3531 (2010).
49. B. Holzmann, Antiinflammatory activities of CGRP modulating innate immune responses in health and disease. *Curr. Protein Pept. Sci.* **14**, 268–274 (2013).

50. W. Zhang *et al.*, Gut-innervating nociceptors regulate the intestinal microbiota to promote tissue protection. *Cell* **185**, 4170–4189.e20 (2022).
51. M. Deen *et al.*, Blocking CGRP in migraine patients–A review of pros and cons. *J. Headache Pain* **18**, 96 (2017).
52. A. F. Russo, D. L. Hay, CGRP physiology, pharmacology, and therapeutic targets: Migraine and beyond. *Physiol. Rev.* **103**, 1565–1644 (2023).
53. S. Wurthmann *et al.*, Impaired wound healing in a migraine patient as a possible side effect of calcitonin gene-related peptide receptor antibody treatment: A case report. *Cephalalgia* **40**, 1255–1260 (2020).
54. C. K. Cullum, M. K. Olsen, H. B. Kocadag, M. Ashina, F. M. Amin, Extreme ecchymoses in a migraine patient using concomitant treatment with calcitonin gene-related peptide receptor antibodies and fish oil supplements: A case report. *BMC Neurol.* **21**, 257 (2021).
55. M. Ruiz, A. Cocores, A. Tosti, P. J. Goadsby, T. S. Monteith, Alopecia as an emerging adverse event to CGRP monoclonal antibodies: Cases series, evaluation of FAERS, and literature review. *Cephalalgia* **43**, 3331024221143538 (2023).
56. U. Reuter, A nasal CGRP receptor antagonist for acute migraine therapy. *Lancet Neurol.* **22**, 190–191 (2023).
57. A. Suekane *et al.*, CGRP-CRLR/RAMP1 signal is important for stress-induced hematopoiesis. *Sci. Rep.* **9**, 429 (2019).
58. X. Gao *et al.*, Nociceptive nerves regulate haematopoietic stem cell mobilization. *Nature* **589**, 591–596 (2021).
59. B. Kurz, B. von Gaudecker, A. Kranz, B. Krisch, R. Mentlein, Calcitonin gene-related peptide and its receptor in the thymus. *Peptides* **16**, 1497–1503 (1995).
60. C. S. N. Klose *et al.*, The neuropeptide neuromedin U stimulates innate lymphoid cells and type 2 inflammation. *Nature* **549**, 282–286 (2017).
61. S. Moriyama *et al.*, Beta(2)-adrenergic receptor-mediated negative regulation of group 2 innate lymphoid cell responses. *Science* **359**, 1056–1061 (2018).
62. H. Yano, D. Artis, Neuronal regulation of innate lymphoid cell responses. *Curr. Opin. Immunol.* **76**, 102205 (2022).
63. N. J. Yang, I. M. Chiu, Bacterial signaling to the nervous system through toxins and metabolites. *J. Mol. Biol.* **429**, 587–605 (2017).
64. J. B. Hernandez *et al.*, The CREB/CRTC2 pathway modulates autoimmune disease by promoting Th17 differentiation. *Nat. Commun.* **6**, 7216 (2015).
65. N. Yoshida *et al.*, ICER is requisite for Th17 differentiation. *Nat. Commun.* **7**, 12993 (2016).
66. J. Talbot *et al.*, Feeding-dependent VIP neuron-ILC3 circuit regulates the intestinal barrier. *Nature* **579**, 575–580 (2020).
67. C. Seillet *et al.*, The neuropeptide VIP confers anticipatory mucosal immunity by regulating ILC3 activity. *Nat. Immunol.* **21**, 168–177 (2020).
68. H. B. Yu *et al.*, Vasoactive intestinal peptide promotes host defense against enteric pathogens by modulating the recruitment of group 3 innate lymphoid cells. *Proc. Natl. Acad. Sci. U.S.A.* **118**, e2106634118 (2021).
69. S. Ibiza *et al.*, Glial-cell-derived neuroregulators control type 3 innate lymphoid cells and gut defence. *Nature* **535**, 440–443 (2016).
70. D. Yang *et al.*, Nociceptor neurons direct goblet cells via a CGRP-RAMP1 axis to drive mucus production and gut barrier protection. *Cell* **185**, 4190–4205.e25 (2022).
71. M. Balood *et al.*, Nociceptor neurons affect cancer immunosurveillance. *Nature* **611**, 405–412 (2022).
72. S. Heinz *et al.*, Simple combinations of lineage-determining transcription factors prime cis-regulatory elements required for macrophage and B cell identities. *Mol. Cell* **38**, 576–589 (2010).
73. Y. Zhou *et al.*, Metascape provides a biologist-oriented resource for the analysis of systems-level datasets. *Nat. Commun.* **10**, 1523 (2019).
74. W. J. Kent *et al.*, The human genome browser at UCSC. *Genome Res.* **12**, 996–1006 (2002).